Trop J Nat Prod Res, August 2025; 9(8): 3831 - 3838 **ISSN 2616-0684 (Print)**
ISSN 2616-0692 (Electronic)

Tropical Journal of Natural Product Research

Available online at https://www.tjnpr.org

Original Research Article

Ultrasonic Wave-Assisted Synthesis of Chalcone Based Pyrazoline Compound and Evaluation of Its Antimicrobial and Cytotoxic Activities

Esti Mulatsari[1]*, Esti Mumpuni[1], Agus Purwanggana[2], Moordiani[1], Diah Kartika Pratami[1], Partomuan Simanjuntak[3]

[1]*Pharmacy Undergraduate Program, Faculty of Pharmacy, Pancasila University, Jakarta, Indonesia*
[2]*Pharmacy Professional Program, Faculty of Pharmacy, Pancasila University, Jakarta, Indonesia*
[3]*Research Center for Pharmaceutical Ingredients and Traditional Medicine, National Research and Innovation Agency (BRIN), Indonesia*

ARTICLE INFO

Article history:
Received 08 June 2025
Revised 10 July 2025
Accepted 13 July 2025
Published online 01 September 2025

ABSTRACT

Chalcone-based pyrazoline compounds are known for their potential antibacterial properties. Previous studies have reported their synthesis via one- or two-step reflux procedures. This study aimed to synthesize and evaluates the antimicrobial and cytotoxic activities of chalcone-based pyrazoline compound. A pyrazoline compound, 4-(1,3-diphenyl-4,5-dihydro-1*H*-pyrazol-5-yl)-N,N-dimethylaniline (PPA), was synthesized through the formation of 4-dimethylamino chalcone (DAC) using a Claisen–Schmidt condensation, followed by cyclization of its α,β-unsaturated carbon system into a pyrazoline ring. Ultrasonic irradiation was used to assist the reaction, employing both one-pot and two-pot synthesis methods. The resulting compounds were evaluated for yield, structural characteristics, antimicrobial activity, and cytotoxicity. Antibacterial activity was assessed through *in silico* molecular docking and *in vitro* minimum inhibitory concentration (MIC) tests. Cytotoxicity was evaluated using the Brine Shrimp Lethality Test (BSLT). Both synthesis methods successfully produced PPA, but TLC analysis revealed that the two-pot method yielded a purer product with a higher yield (99%). The antimicrobial activity evaluation showed that both DAC and PPA exhibited weak antimicrobial activity, with MIC values of 5000 µg/mL against *Escherichia coli*, *Staphylococcus aureus*, *Salmonella typhi*, and *Candida albicans*. In the cytotoxicity assay, PPA exhibited significantly lower toxicity (LC_{50} = 81.27 µg/mL) than DAC (LC_{50} = 0.0042 µg/mL). These findings suggest that conversion of the *α,β*-unsaturated system to a pyrazoline ring structure reduces the compound's cytotoxicity.

Keywords: Chalcone, Pyrazoline, Synthesis, Antimicrobial, Cytotoxicity.

Introduction

Drug development through the structural modification of natural compounds or secondary metabolites has progressed rapidly in recent years.[1–3] One of the most commonly modified scaffolds is chalcone. Chalcone, or 1,3-diphenyl-2E-propen-1-one, is a compound characterized by a benzylidene acetophenone core, consisting of two aromatic rings connected by an α,β-unsaturated carbonyl system. This structure makes chalcones valuable intermediates for the synthesis of flavones and flavanones, which are known for their wide range of biological activities.[4,5] Chalcones can be synthesized via several methods, including the Suzuki coupling, Fries rearrangement, and Friedel–Crafts acylation. However, the Claisen–Schmidt condensation is the most widely used, involving the reaction of acetophenone or its derivatives with benzaldehyde derivatives in the presence of strong base catalysts (e.g., NaOH, KOH, $Ba(OH)_2$, or $LiOH{\cdot}2H_2O$), or acid catalysts such as $AlCl_3$, BF_3–Et_2O, $TiCl_4$, or $RuCl_3$.[6]

*Corresponding author. Email: esti.mulatsari@univpancasila.ac.id
Tel.: +6285729086842

Citation: Mulatsari E, Mumpuni E, Purwanggana A, Moordiani, Pratami DK, Simanjuntak P. Ultrasonic Wave-Assisted Synthesis of Chalcone Based Pyrazoline Compound and Evaluation of Its Antimicrobial and Cytotoxic Activities. Trop J Nat Prod Res, 2025; 9(8): 3831 – 3838 https://doi.org/10.26538/tjnpr/v9i8.43

Official Journal of Natural Product Research Group, Faculty of Pharmacy, University of Benin, Benin City, Nigeria

Numerous chalcone derivatives have demonstrated diverse biological activities. For example, halogenated and methylated chalcones have shown anti-obesity effects,[7] coumarin-chalcones possess antidiabetic properties,[8] and triazole-linked chalcones have exhibited anticancer potential,[9] Other modifications, such as piperidine substitution, enhance antioxidant activity,[10] while chlorination increases antibacterial potency. Electron-withdrawing groups tend to enhance antibacterial activity, while electron-donating groups (e.g., p-CH_3, OCH_3) reduce it. Moreover, the position of substitution on the aromatic ring significantly affects biological activity. For example, antibacterial activity follows the trend 2,4-Cl_2 > p-Cl > m-Cl > o-Cl.[11]

The global rise in bacterial and fungal infections has led to growing concerns regarding antimicrobial resistance, which contributes to treatment failure, increased mortality, and higher healthcare costs.[12,13] Developing novel antibacterial agents is therefore critical. One strategy is to modify existing bioactive structures to improve their efficacy.[14,15] Fluorinated chalcones, for instance, have shown enhanced activity against *Staphylococcus epidermidis*, *Escherichia coli*, and *Pseudomonas aeruginosa*.[16] Chlorinated chalcone has been reported to enhance antibacterial activity against *Staphylococcus aureus*.[11] Modification with the addition of halogens, besides increasing the antibacterial effectiveness, also increases the toxicity of the compound.[17] Recent studies have focused on more complex chalcone derivatives, including those fused with ferrocene, steroids, pyrazoline, or thiazolidine structures. Among these, pyrazoline-based chalcones have shown promising antibacterial properties. Traditionally, the synthesis of pyrazoline chalcones has been conducted via two-step reflux methods, often requiring long reaction times and varying conditions. Optimizing these reactions is essential to improving efficiency and yield.[18–22] The use of ultrasonic waves for synthesis has been widely used in previous research and is able to accelerate the synthesis process of curcumin and curcumin analogues.[23,24]

In the development of pyrazole compounds, ultrasonication has been applied to the synthesis of N-[[3-(4-bromophenyl)-1*H*-pyrazol-5-

yl]carbamothioyl]-4-chloro-benzamide,[25] ethyl 1-(2,4-dichlorophenyl)-1*H*-pyrazole-3-carboxylates[26] and various other pyrazole derivatives able to accelerate reactions within 10-20 minutes.[25,27] Exposure to ultrasonic waves through a medium will produce vibrations. The propagation medium with liquid is known as an ultrasonic bath. Vibrations will provide intensive stirring to the reaction process. This is what causes synthesis with exposure to ultrasonic waves with the right frequency to be accelerated.

In this study, the synthesis of pyrazoline derivatives based on chalcone structures using both one-pot and two-pot methods under ultrasonic irradiation was investigated. The conversion of the *α,β*-unsaturated carbon system of 4-dimethylamino chalcone (DAC) to a pyrazoline ring is expected to enhance antibacterial activity while reducing polarity, thereby improving cell membrane permeability. The use of ultrasonic waves is also intended to accelerate reaction rates and improve yield. Previous research has shown that ultrasonication significantly reduces reaction time in the synthesis of curcumin analogue and various pyrazole derivatives. Identification and characterisation of the resulting compound was done. Antimicrobial activity test was performed *in silico* using molecular docking tool to determine the mechanism of bacterial inhibition, and *in vitro* to determine the Minimum Inhibitory Concentration (MIC) in Gram-positive and Gram-negative bacteria. The Cytotoxicity test was carried out using Brine Shrimp Lethal Test (BSLT).

Materials and Methods

Chemicals

The reagents used in this study included acetophenone, phenylhydrazine, ethanol, 4-dimethylaminobenzaldehyde, hydrochloric acid, n-hexane, ethyl acetate, DMSO, TLC plates, and distilled water. All chemicals were of pro analysis (PA) grade and used without further purification.

Synthesis of compounds

One pot synthesis of PPA

The one-pot synthesis of PPA was initiated by adding 4-dimethylaminobenzaldehyde to a glass beaker containing acetophenone in 10 mL of ethanol and 3 mL of 50% NaOH. The mixture was homogenized using ultrasonic irradiation until the formation of 4-dimethylamino chalcone (DAC) was observed. Phenyl hydrazine was then added dropwise in a 1:1:1 molar ratio (4-dimethylaminobenzaldehyde: acetophenone: phenylhydrazine). The reaction mixture was subjected to ultrasonication at 40°C for 20 minutes at a frequency of 40 kHz. The resulting product was crystallized using cold distilled water, and the pH was adjusted to neutral with HCl.[28,29]

Two pot synthesis of PPA

The two-pot synthesis began with the formation of DAC. First, 0.01 mol of 4-dimethylaminobenzaldehyde (DAB) was dissolved in 10 mL of ethanol, followed by the sequential addition of 3 mL of 50% NaOH and 0.01 mol of acetophenone. The mixture was irradiated with ultrasonic waves for 10 minutes. The crude product was precipitated using cold distilled water and neutralized with HCl. In the second stage, 0.61 g of DAC was dissolved in 10 mL of ethanol, and 240 µL of phenyl hydrazine was added.. The reaction mixture was ultrasonicated for 20 minutes, and the final product was isolated by crystallization with cold distilled water and then neutralized with 2 N hydrochloric acid.[29,30]

Compound identification and characterization

The synthesized compounds were evaluated organoleptically for physical properties such as colour, shape, and odour. Instrumental characterization included melting point determination, UV-Vis spectroscopy, thin-layer chromatography (TLC), infrared (IR) spectroscopy, liquid chromatography-Mass spectrometry (LC-MS), and Proton and carbon-13 nuclear magnetic resonance (^{1}H-NMR and ^{13}C-NMR) spectroscopy. Melting point was measured using open capillary tubes. IR spectra were obtained using a Shimadzu FTIR spectrophotometer. TLC was performed on silica gel plates using a 3:1 mixture of n-hexane:ethyl acetate as the mobile phase. Spots were visualized under UV light at 254 nm and 366 nm, and Rf values were calculated. UV-Vis spectra were recorded at the maximum absorption wavelengths of each compound. LC-MS analysis was performed with a MassLynx LC-MS/MS QTof instrument. Structural confirmation was further supported by ^{1}H-NMR and ^{13}C-NMR (Bruker Avance Neo-Ascend).

In silico antibacterial activity test

The *in silico* antibacterial activity was evaluated through molecular docking using Molegro Virtual Docker (MVD) to assess the binding affinity of the synthesized ligands (PPA and DAC) toward selected target proteins. The PPA structure was constructed using ChemDraw and subsequently subjected to energy minimization employing the MMFF96 force field algorithm. The target proteins used for the docking included 1HNJ (*β*-ketoacyl-acyl carrier protein synthase III, FabH), 3MZD (penicillin-binding protein, PBP), and 6O9S (ribosomal subunit of *Staphylococcus aureus*). Amoxicillin was employed as a reference compound for comparative purposes. Docking protocol validation was performed by calculating the root mean square deviation (RMSD) following redocking of each protein's native ligand.

Evaluation of antimicrobial activity in vitro (Minimum Inhibitory Concentration Determination)

The antimicrobial activity of the synthesized compounds was evaluated against standard bacterial strains, including *Staphylococcus aureus* ATCC 6538, *Escherichia coli* ATCC 8739, and *Salmonella typhii* ATCC 14028, as well as against the standard yeast strain *Candida albicans* ATCC 10231. The antimicrobial activity of the newly synthesized pyrazoline derivatives against bacteria and fungi was assessed using the microdilution method according to the guidelines of the Clinical and Laboratory Standards Institute (CLSI). Microbial inocula were prepared by harvesting colonies of *Escherichia coli (Ec), Staphylococcus aureus (Sa), Salmonella typhii (St), and Candida albicans (Ca)* aged 24 hours (for bacteria) and 2–3 days (for fungi). A single dose of the mixed microbial colonies was suspended in 0.9% NaCl solution and homogenized. The optical density (OD) of the suspension was adjusted using UV-Vis spectrophotometry at a wavelength of 600 nm to an absorbance of 0.1 ± 0.02, corresponding to approximately 1 x 10^8 CFU/mL for bacteria and 1 x 10^6 CFU/mL for fungi. The MIC test was conducted using compound concentrations ranging from 10,000 to 256 µg/mL dissolved in concentrated DMSO, with TSB (Tryptic Soy Broth) used for subsequent dilutions. For the treatment group, 1 mL of the sample solution was mixed with 0.5 mL of the microbial inoculum. The following controls were prepared: Negative control (TSB): 1 mL of TSB mixed with 0.5 mL of microbial inoculum, Negative control (solvent): 1 mL of solvent mixed with 0.5 mL of microbial inoculum, Positive control (antibiotics): 1 mL of antibiotic solution (amoxicillin, cefadroxil, or nystatin) mixed with 0.5 mL of microbial inoculum. All sample tubes were incubated at 30–35°C for 24 hours for bacterial strains, and at 20–25°C for 48–72 hours for the fungal strain (*C. albicans*). The turbidity of each sample was observed and compared before and after incubation. Subsequently, samples, negative controls, and positive controls were streaked onto TSA (Tryptic Soy Agar) for bacteria and SDA (Sabouraud Dextrose Agar) for fungi. TSA plates were incubated at 30–35°C for 24 hours, and SDA plates at 20–25°C for 48–72 hours. Colony growth was then assessed. The presence of microbial colonies indicated a lack of inhibitory activity, whereas the absence of colony growth indicated effective antimicrobial activity of the sample.[15,31]

Cytotoxicity test

Approximately 50 mg of *Artemia salina Leach* shrimp eggs were hatched in a dual-chamber system consisting of dark and light vessels filled with synthetic seawater, prepared by dissolving 38 g of non-iodized salt in 1 litre of distilled water. The dark chamber contained the eggs and an aerator, while the light chamber was illuminated with an 18-watt fluorescent lamp for 48 hours to facilitate hatching. A test solution was prepared by dissolving 50 mg of the sample in 5 mL of solvent to produce a stock solution with a concentration of 10,000 ppm. From this stock, eight serial dilutions were made to obtain test concentrations of 1000, 500, 250, 100, 50, 25, 12.5, and 6.25 ppm. Each concentration was tested in triplicate. Control solutions using DMSO at concentrations of 10%, 5%, and 2.5% were also prepared as stock

solutions of 10,000 ppm. These were then diluted to produce control concentrations of 1000, 500, and 250 ppm, respectively. For each test and control solution, 10 *A. salina* leach larvae were introduced into each replicate. Observations were made after 24 hours of exposure. The number of live and dead larvae in each concentration group was recorded. The mortality data were then analyzed using probit analysis to determine the LC_{50} value. The results from the test solutions were compared with the corresponding control groups.[32]

Results and Discussion

Synthesis and TLC profile of DAC and PPA

The synthesis of the target compound PPA began with the formation of the intermediate DAC through a Claisen–Schmidt condensation reaction. Acetophenone reacted with sodium hydroxide in ethanol to form a carbanion, which then reacted with 4-dimethylaminobenzaldehyde to yield the α,β-unsaturated chalcone structure. Subsequently, DAC was cyclized with phenyl hydrazine to form the pyrazoline ring, producing a compound with three aromatic rings. The synthesis scheme of DAC and PPA is presented in Figure 1. The thin-layer chromatogram (Figure 2) showed that PPA (spots C and D) exhibited a higher Rf value compared to DAC (spot B), confirming the reduced polarity of pyrazoline compared to the chalcone precursor. The TLC profile under 366 nm UV light revealed distinct fluorescence: DAC appeared yellow, while PPA appeared blue. The two-pot synthesis method produced a single spot, indicating a purer compound, while the one-pot method showed a minor impurity (residual DAC). Organoleptic examination of the compounds on the TLC chromatogram showed that DAC had an orange-yellow colour, while PPA had a brownish-orange colour. Both compounds emitted an aromatic odour. The calculation of the yield indicated that the two-pot method produced a higher yield and a purer product than the one-pot method (Table 1).

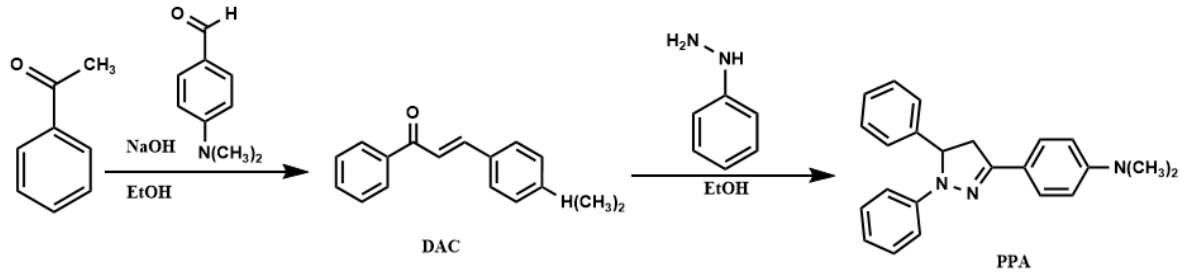

Figure 1: Synthesis scheme of 4-dimethylamino chalcone (DAC) and 4-(1,3-diphenyl-4,5-dihydro-1*H*-pyrazol-5-yl)-N,N-dimethylaniline (PPA)

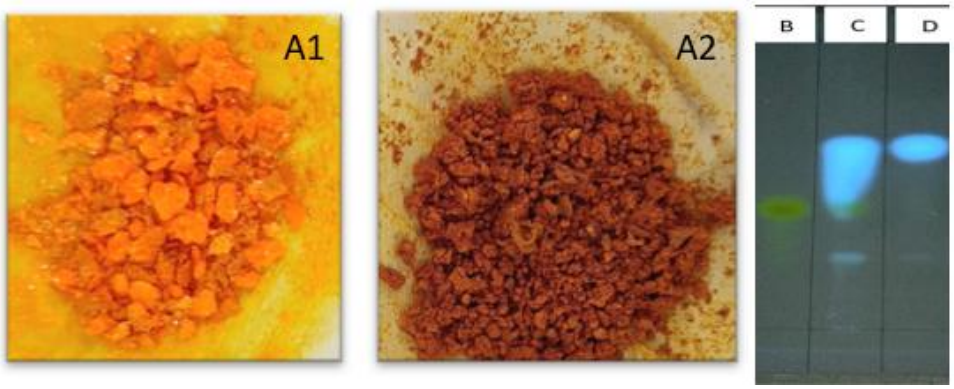

Figure 2: Physical appearance and TLC profile of synthesized compounds; 4-dimethylamino chalcone (DAC) (**A1)** and 4-(1,3-diphenyl-4,5-dihydro-1*H*-pyrazol-5-yl)-N,N-dimethylaniline (PPA) (**A2)**; **(B):** DAC; **(C):** PPA (one-pot); **(D):** PPA (two pot)

Characterization of DAC and PPA

UV-Vis spectral data

The compound DAC exhibited two main absorption peaks: one at 264 nm ($\pi \rightarrow \pi^*$ transition in the UV region) and another at 418 nm (visible region), associated with the extended conjugated system of the *α,β*-unsaturated carbon (Table 2). The UV-Vis spectra of PPA (from both one-pot and two-pot synthesis) showed three absorption peaks at 204, 254, and ~356–358 nm, indicative of $\pi \rightarrow \pi^*$ and $n \rightarrow \pi^*$ transitions, consistent with substituted aromatic and heterocyclic systems (Table 2).[30,33]

FTIR, LC-MS, and ¹H-NMR spectral data

The FTIR, LC-MS and ¹H-NMR spectra of DAC and PPA are presented in the supplementary Information. Identification using FTIR was conducted to determine the functional groups present in the synthesized compounds. Identification using FTIR, LC-MS, and ¹H- & ^{13}C-NMR, as well as antimicrobial activity and toxicity tests, were carried out on DAC and PPA compounds synthesized using the two-pot method. The FTIR spectrum of 4-dimethylamino chalcone (DAC) showed absorption bands at 1741 cm^{-1}, corresponding to C=O (carbonyl) bond vibrations; and at 1430 cm^{-1}, indicating aromatic C=C bond vibrations. The absorption band at 3656.81 cm^{-1} can be ascribed to O-H vibration of the residual solvent (ethanol) molecules. The FTIR spectrum of the pyrazoline derivative (PPA) displayed similar absorption bands as the 4-dimethylamino chalcone (DAC), except for the absence of absorption around 1700 cm^{-1}. The absence of the vibration around 1700 cm^{-1} indicates the loss of the carbonyl (C=O) group, which suggests that the compound has been successfully converted into a pyrazoline derivative.[30,33–38]. The IR spectrum of pyrazoline derivatives, was characterized by the presence of an imine group (C=N) detected at wave numbers 1550-1600 cm^{-1}.[39] In the region between 1500–400 cm^{-1}, the PPA spectrum showed a large and irregular fluctuations, indicating the higher structural complexity of the compound. LC-MS analysis confirmed the formation of the target compound (PPA); however, the presence of multiple peaks at different retention times (Rt) indicated that several side products were also formed.

Table 1: Thin layer chromatography (TLC) data of synthesized compounds

Spot	Compound	Rf	AUC (%)
B	DAC	0.51	93.34
C	PPA (one-pot)	0.77	86.38
D	PPA (two-pot)	0.78	99.00

PPA: 4-(1,3-diphenyl-4,5-dihydro-1*H*-pyrazol-5-yl)-N,N-dimethylaniline; DAC: 4-dimethylamino chalcone

Table 2: UV-Visible spectral data of synthesized compounds

Compound	Wavelenght of maximum absorption (λ_{max}) (nm)	
	Ultra violet	Visible
DAC	264	418
PPA (one-pot)	204	
	254	-
	358	
PPA (two-pot)	204	
	254	-
	356	

PPA: 4-(1,3-diphenyl-4,5-dihydro-1*H*-pyrazol-5-yl)-N,N-dimethylaniline; DAC: 4-dimethylamino chalcone

Compound DAC was identified with an *m/z* value of 252 $[M+H]^+$ consistent with the molecular formular $C_{17}H_{17}NO$ at a retention time of 11.87 minutes, while the pyrazoline compound was detected with an *m/z* value of 342 $[M+H]^+$ corresponding to $C_{23}H_{23}N_3$ molecule at a retention time of 14.05 minutes. The ^{1}H-NMR and ^{13}C-NMR spectroscopic analysis of DAC exhibited a consistent spectral pattern whose data is presented in Table 3.

Table 3: ^{1}H- and ^{13}C-NMR chemical shifts of 4-dimethylamino chalcone (DAC)

No	^{13}C-NMR CD_3OD, 125 MHz	^{1}H-NMR CD_3OD, 500 MHz
1	138.73	-
2	130.45	8.05 (m)
3	128.30	7.63 (m)
4	132.26	7.54 (m)
5	128.30	7.63 (m)
6	130.45	8.05 (m)
7	122.35	-
8	129.99	7.55 (m)
9	111.62	6.79 (m)
10	152.65	-
11	111.62	6.79 (m)
12	129.99	7.55 (m)
1’	115.76	7.49 (d, *J* = 15.0 Hz)
2’	146.65	7.52 (d, *J* = 15.0 UHz)
3’ C=O	191.35	-
N-Me_1	38.82	3.05 (s)
N-Me_2	38.82	3.05 (s)

The chemical shifts between δH 7.63 ~ 8.05 are for the protons of the aromatic ring A, and δH 6.79 ~ 7.55 are for the protons of the aromatic ring B. The vinylic protons of the chalcone moiety (–CH=CH–CO–) typically appear at δH 7.49 (d, *J* = 15.0 Hz; H-1’) and δH 7.52 (d, *J* = 15.0 Hz; H-2’) showing *trans* stereochemistry. Investigation based on ^{13}C-NMR spectrum showed that there were 17 carbon atoms consisting of eleven methine carbons; three quarternary carbons, one carbonyl carbon and two methyl carbons.

The ^{1}H-NMR and ^{13}C-NMR analysis of PPA displayed spectral data (Table 4) that was consistent with the proposed structure. The protons of aromatic ring A appeared at δH 7.18 (m); 7.40 (m) and 7.77 (m). The protons of aromatic ring B appeared at δH 6.72 (m); 6.77 (m) and 7.13 (m). The protons of aromatic ring C appeared at δH 6.77 and δH 7.13 ppm. The $N(CH_3)_2$ group protons appeared as a singlet at δH 2.91 ppm. The chemical shift for the pyrazole ring proton were at δH 5.25 (dd, *J* = 5.0; 10.0 Hz; H-4’) and δH 2.91 (s, br; H-5’). Interpretation of ^{13}C-NMR and Distortionless Enhancement Polarizzation Transfer (DEPT) spectra gave 23 carbons consisting of one (-CH_2-); one (-CH-); two (-CH_3); 14 (-CH=) and five (-C=).

Table 4: ^{1}H- and ^{13}C-NMR chemical shifts of 4-(1,3-diphenyl-4,5-dihydro-1*H*-pyrazol-5-yl)-N,N-dimethylaniline (PPA)

No.	^{13}C-NMR (CD_3OD, 175 MHz)	^{1}H-NMR (CD_3OD, 700 MHz)
1	133.01 (s)	-
2	125.34 (d)	7.77 (m)
3	128.18 (d)	7.40 (m)
4	126.40 (d)	7.18 (m)
5	128.18 (d)	7.40 (m)
6	125.34 (d)	7.77 (m)
7	145.14 (s)	-
8	113.32 (d)	6.77 (m)
9	128.21 (d)	7.13 (m)
10	118.47 (d)	6.72 (m)
11	128.21 (d)	7.13 (m)
12	113.32 (d)	6.77 (m)
13	130.92 (s)	-
14	128.21 (d)	7.13 (m)
15	113.32 (d)	6.77 (m)
16	147.05 (s)	-
17	113.32 (d)	6.77 (m)
18	128.21 (d)	7.13 (m)
N-Me_1	43.06 (q)	3.33 (s)
N-Me_2	43.06 (q)	3.33 (s)
1’	150.33 (s)	-
2’-N	-	-
3’ -N	-	-
4’	64.14	5.25 (dd)
5’	39.66	2.91 (s,br)

Antimicrobial activity of DAC and PPA

Antimicrobial activity evaluation using *in vitro* assay was conducted by determining the minimum inhibitory concentration of each compound synthesized. The MIC assay showed that both DAC and PPA (from both synthesis methods) inhibited the growth of *E. coli*, *S. aureus*, *S. typhii*, and *C. albicans* only at relatively high concentrations (MIC = 5000

µg/mL). These results indicate weak antimicrobial potency, especially when compared to known pyrazoline derivatives with halogen or hydroxyl substituents.[11,17]

Antimicrobial activity evaluation using *in silico* methods was aimed at determining the mechanism of action of the compounds as antimicrobial agents. Validation of the molecular docking protocol was carried out by determining the RMSD value of each combination of algorithms and scoring functions used as shown in Table 5.

Superimposition of the redocking pose of native ligand and the natural pose is shown in Figure 3. The three bacterial receptors used include the PDB IDs 1HNJ (beta-Ketoacyl-acyl carrier protein synthase III (FabH)), 3MZD (Penicillin-binding proteins (PBPs)), and 6O9S (ribosomal sub unit of *S. aureus*). The results of the *in silico* study showed that PPA had weaker antibacterial activity compared the reference drug (amoxicillin), the rerank scores of both compounds are presented in Table 6. Figure 4 represents the visualization of the interactions between the ligand and amino acid residues of the receptors. The visualized interactions revealed that PPA formed only two hydrogen bonds, along with several alkyl interactions on interaction with 1HNJ (*β*-ketoacyl-acyl carrier protein synthase III, FabH), and 3MZD (penicillin-binding proteins, PBPs).

Table 5: The best docking protocol of each receptor

PDB ID	Algorithm	Scoring Function	Coordinate	Radius	Best RMSD
3MZD	Moldock Score	Moldock SE	44.05; 6.45; 29.12	10	2.18
1HNJ	Moldock Score	Moldock Optimizer	26.73; 13.6; 32.68	15	6.4
6O9S	Moldock Score	Moldock SE	66.96;76.71; 150.54	10	1.58

Table 6: Rerank scores of test compounds

PDB ID	Native Ligand	Amoxicillin	DAC	PPA
3MZD	-81.76	-94.82	-68.97	-86.43
6O9S	-68.73	-82.11	-67.46	-75.74
1HNJ	-121.81	-95.67	-70.90	-89.11

PPA: 4-(1,3-diphenyl-4,5-dihydro-1*H*-pyrazol-5-yl)-N,N-dimethylaniline; DAC: 4-dimethylamino chalcone

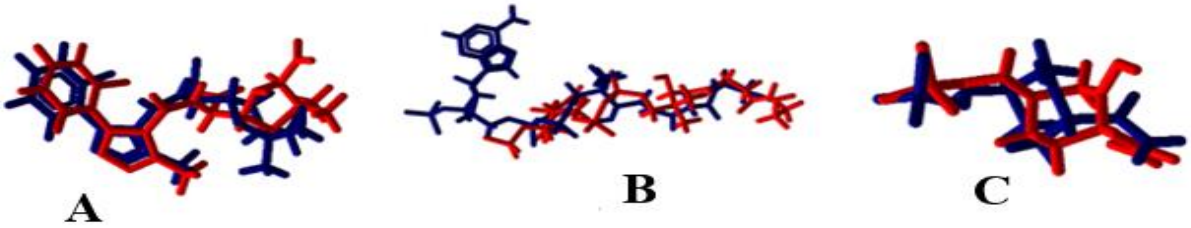

Figure 3: Superimposed poses of native ligand and native ligand redocking; **(A):** 3MZD, **(B):** 1HNJ, and **(C):** 6O9S

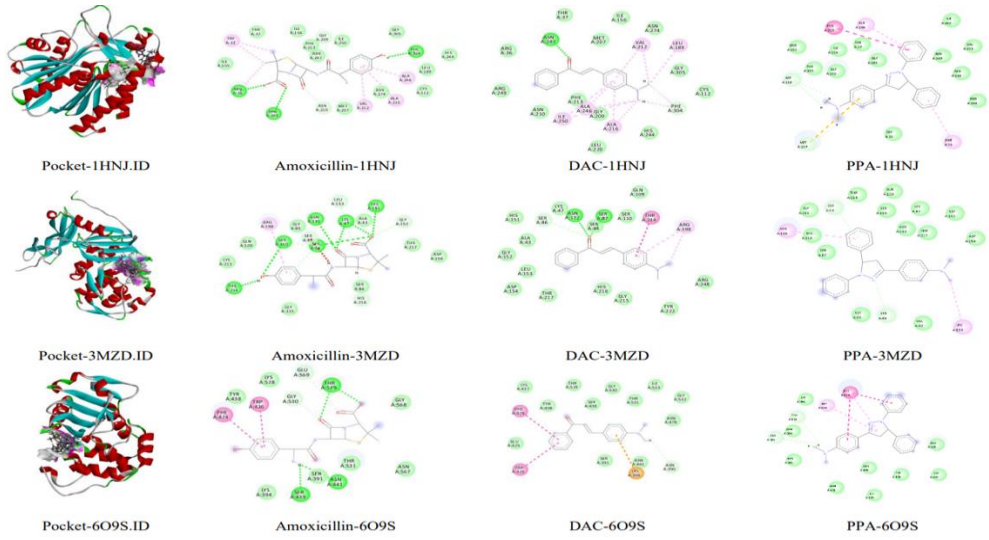

Figure 4: Visualization of the interaction of compounds with amino acid residues of receptors

In contrast, amoxicillin formed three and six hydrogen bonds with these targets, respectively. Meanwhile, the interaction between PPA and 6O9S (ribosomal subunit of *S. aureus*) have two hydrogen bonding beside Van Der Waal and Pi-Pi alkyl interactions that influenced affinity. This causes the pyrazoline compound not to bind strongly to the bacterial receptor so that it is unable to inhibit bacterial growth effectively.

Cytotoxic activity of DAC and PPA

Cytotoxicity test was carried out using the BSLT method by calculating the percentage of death and probit analysis in several series of test solution concentrations until the LC_{50} value could be determined. Tables 7 and 8 show the raw data for calculating the LC_{50}. The LC_{50} values for DAC and PPA were 0.0042 and 81.2710 µg/mL, respectively based on percentage death and 0.2214 and 60.9592 µg/mL, respectively based on probit calculations. This value indicates that both compounds have high cytotoxic properties. The LC_{50} values obtained showed that changing the *α-β* unsaturated carbon atoms in chalcone to pyrazoline reduced the cytotoxic activity.

Table 7: Cytotoxicity of 4-dimethylamino chalcone (DAC)

Doses (D) (ppm)	Log D (x)	Death	Live	Δ Death	Δ Live	Death/Live	% mortality (y)	Probit
1,001.20	3.00	30	0	228	0	228/228	100.00	8.0900
500.60	2.70	30	0	198	0	198/198	100.00	8.0900
250.30	2.40	30	0	168	0	168/168	100.00	8.0900
100.12	2.00	30	0	138	0	138/138	100.00	8.0900
50.06	1.70	30	0	108	0	108/108	100.00	8.0900
25.03	1.40	30	0	78	0	78/78	100.00	8.0900
12.52	1.10	26	4	48	4	48/52	92.31	6.4317
6.26	0.80	22	8	22	12	22/34	64.71	5.3813

Table 8: Cytotoxicity of 4-(1,3-diphenyl-4,5-dihydro-1*H*-pyrazol-5-yl)-N,N-dimethylaniline (PPA)

Dose (D) (ppm)	Log D (x)	Death	Live	Δ Death	Δ Live	Death/Live	% mortality (y)	Probit
1,001.20	3.00	30	0	114	0	114/114	100.00	8.0900
500.60	2.70	30	0	84	0	84/84	100.00	8.0900
250.30	2.40	19	11	54	11	54/65	83.08	5.9532
100.12	2.00	19	11	35	22	35/57	61.40	5.2920
50.06	1.70	6	24	16	46	16/62	25.81	4.3543
25.03	1.40	4	26	10	72	10/82	12.20	3.8300
12.52	1.10	3	27	6	99	6/105	5.71	3.4239
6.26	0.80	3	27	3	126	3/129	2.33	3.0061

Conclusion

The compounds DAC and PPA synthesized using ultrasonic-assisted method exhibited weak antimicrobial activity, with minimum inhibitory concentrations (MIC) of 5000 µg/mL against *Escherichia coli*, *Staphylococcus aureus*, *Salmonella typhii*, and *Candida albicans*. Molecular docking analysis revealed that PPA had lower binding affinity and formed fewer hydrogen bonds with bacterial targets compared to the reference drug (amoxicillin), supporting the observed low antimicrobial activity. In terms of cytotoxicity, PPA demonstrated a significantly higher LC_{50} value (81.27 µg/mL) than DAC (0.0042 µg/mL), indicating that structural modification by converting the *α,β*-unsaturated chalcone into a pyrazoline ring can reduce cytotoxicity. These findings suggest that while PPA has limited antibacterial potential, it may serve as a less toxic precursor for further structural optimization aimed at enhancing biological activity.

Conflict of Interest

The authors declare no conflict of interest.

Author's Declaration

The authors hereby declare that the work presented in this article is original and that any liability for claims relating to the content of this article will be borne by them.

Acknowledgements

The authors would like to thank the Ministry of Education, Culture, Research, Technology and Higher Education for the research grant provided through the regular fundamental grant programme with contract number: 105/E5/PG.02.00.PL/2024; 817/LL3/AL.04/2024; 0046/LPPM/UP/VI/2024.

References

1. Mumpuni E, Purwanggana A, Mulatsari E, Rasdianti P. Synthesis of 1,5-Bis(3'-Ethoxy-4'-Hydroxyphenyl)-1,4-Pentadien-3-one (EHP) Compound Using Technical Grade Ethyl Vanillin as Raw Material. J Zarah. 2021; 9(1):29–35.
2. Purwanggana A, Mulatsari E, Mumpuni E, Kusumaningtyas SMD. Anti-Acne Gel Formulation With 1, 5-Bis (3'-Etoxy-4'-Hydroxyphenyl)-1, 4-Pentadiene-3-On (EHP) As an Antibacterial Ingredient. J Ilmu Kefarmasian Indones. 2021; 19(2):216–225.
3. Mumpuni E, Mulatsari E, Puwanggana A, Vicy SF. Chemical Reaction Kinetics of 1,5-Bis (3'-Ethoxy-4'-Hydroxyphenyl)-1,4– Pentadient-3–one Synthesis with Food Grade Raw Material. Int J Appl Pharm. 2021; 13(Special Issue 2):173-177.
4. Goyal K. Chalcones: A Review on Synthesis and Pharmacological Activities. J Appl Pharm Sci. 2021; 11(1):1–14.
5. Singh P, Anand A, Kumar V. Recent Developments in Biological Activities of Chalcones: A Mini Review. Eur J Med Chem. 2014; 85:758–777.
6. Nasir S, Bukhari A, Jasamai M, Jantan I, Ahmad W. Review of Methods and Various Catalysts Used for Chalcone Synthesis. Mini Rev Med Chem. 2013; 10(1):73–83.
7. Hsieh CT. 2-Bromo-4′-Methoxychalcone and 2-Iodo-4′-Methoxychalcone Prevent Progression of Hyperglycemia and Obesity via 5′-Adenosine-Monophosphate-Activated Protein Kinase in Diet-Induced Obese Mice. Int J Mol Sci. 2018; 19(9):2841.
8. Konidala SK, Kotra V, Danduga RCSR, Kola PK. Coumarin-Chalcone Hybrids Targeting Insulin Receptor: Design, Synthesis, Anti-Diabetic Activity, and Molecular Docking. Bioorg Chem. 2020; 104:104273.
9. Chinthala Y. Synthesis, Docking and ADMET Studies of Novel Chalcone Triazoles for Anti-Cancer and Anti-Diabetic Activity. Eur J Med Chem. 2015; 93:564–573.
10. Haq IU, Ali I, Salar U, Chigurupati S, Qureshi U, Almahmoud SA, Hameed S, Konanki S, Ahmad M, Ali M, Haq ZU, Khan KM. Synthetic Piperidine-Substituted Chalcones as Potential Hits for α-Amylase Inhibitory and Antioxidant Activities. Future Med Chem. 2023; 15(6):497–515.
11. Chen ZH, Zheng CJ, Sun LP, Piao HR. Synthesis of New Chalcone Derivatives Containing a Rhodanine-3-Acetic Acid Moiety with Potential Anti-Bacterial Activity. Eur J Med Chem. 2010; 45(12):5739–5743.
12. Bush K, Courvalin P, Dantas G, Davies J, Eisenstein B, Huovinen P, Nightingale L, Srinivasan A, Stokes B, Viswanathan V, Wagar E, Walsh F. Tackling Antibiotic Resistance. Nat Rev Microbiol. 2011; 9(12):894–896.
13. Levy SB and Marshall B. Antibacterial Resistance Worldwide: Causes, Challenges and Responses. Nat Med. 2004; 10(12S):S122–S129.
14. Mumpuni E, Purwanggana A, Mulatsari E. New Antibacterial Agents from Curcumin Derivative Compounds. Bogor: PT. Idemedia Pustaka Utama; 2019:1–70.
15. Purwanggana A, Mumpuni E, Mulatsari E. *In Vitro* and *In Silico* Antibacterial Activity of 1.5-Bis (3'-Ethoxy-4'-Hydroxyphenyl)-1-4-Pentadiene-3-One. Int J Pharm Pharm Sci. 2018; 10(5):3–9.
16. Yadav P, Lal K, Kumar L, Kumar A, Kumar A, Paul AK, Sharma SK, Lal J. Synthesis, Crystal Structure and Antimicrobial Potential of Some Fluorinated Chalcone-1,2,3-Triazole Conjugates. Eur J Med Chem. 2018; 155:263–274.
17. Xu M, Wu P, Shen F, Ji J, Rakesh KP. Chalcone Derivatives and Their Antibacterial Activities: Current Development. Bioorg Chem. 2019; 91:103133.
18. Hassan AS and Hafez TS. Antimicrobial Activities of Ferrocenyl Complexes: A Review. J Appl Pharm Sci. 2018; 8(5):156–165.
19. Kakati D, Sarma RK, Saikia R, Barua NC, Sarma JC. Rapid Microwave Assisted Synthesis and Antimicrobial Bioevaluation of Novel Steroidal Chalcones. Steroids. 2013; 78(3):321–326.
20. Farooq S and Ngaini Z. One-Pot and Two-Pot Synthesis of Chalcone Based Mono and Bis-Pyrazolines. Tetrahedron Lett. 2020; 61(4):151416.
21. Nakamura C, Kawasaki N, Miyataka H, Jayachandran E, Kim IH, Kirk KL, Taguchi T. Synthesis and Biological Activities of Fluorinated Chalcone Derivatives. Bioorg Med Chem. 2002; 10(3):699–706.
22. Sun J, Li M, Lin M, Zhang B, Chen X. High Antibacterial Activity and Selectivity of the Versatile Polysulfoniums that Combat Drug Resistance. Adv Mater. 2021; 33(41):2102148.
23. Pramuna BS and Kurnawati H. Isolasi Kurkumin Dalam Kunyit Dengan Metode Solven Ekstraksi Ultrasonik. 2020; 23–24.
24. Nur Anisa D, Anwar C, Afriyani H. Synthesis of Curcumin Analog Compounds Based on Veratraldehyde Using Ultrasound Method. Anal Anal Environ Chem. 2020; 5(01):74–81.
25. Nitulescu GM, Matei L, Aldea IM, Draghici C, Olaru OT, Bleotu C. Ultrasound-Assisted Synthesis and Anticancer Evaluation of New Pyrazole Derivatives as Cell Cycle Inhibitors. Arab J Chem. 2019; 12(6):816–824.
26. Machado P, Lima GR, Rotta M, Bonacorso HG, Zanatta N, Martins MAP. Efficient and Highly Regioselective Synthesis of Ethyl 1-(2,4-Dichlorophenyl)-1H-Pyrazole-3-Carboxylates Under Ultrasound Irradiation. Ultrason Sonochem. 2011; 18(1):293–299.
27. Dofe VS, Sarkate AP, Shaikh ZM, Jadhav CK, Nipte AS, Gill CH. Ultrasound-Assisted Synthesis of Novel Pyrazole and Pyrimidine Derivatives as Antimicrobial Agents. J Heterocycl Chem. 2018; 55(3):756–762.
28. Farooq S and Ngaini Z. One-Pot and Two-Pot Synthesis of Chalcone Based Mono and Bis-Pyrazolines. Tetrahedron Lett. 2020; 61(4):151416.
29. Farooq S and Ngaini Z. Chalcone Derived Pyrazole Synthesis via One-Pot and Two-Pot Strategies. Curr Org Chem. 2020; 24(13):1480-1493.
30. Puspita A, Teruna HY, Jasril. Synthesis of Pyrazoline from 3-Chloro Naphthalene Core Chalcone and Test of Its Activity as an Antibacterial. Jom Fmipa. 2014; 1(2):403–410.
31. Mumpuni E, Mulatsari E, Purwanggana A, Paramita IP. New Antibacterial Agents from Curcumin Derivative Compounds. Bogor: Idemedia Pustaka Utama; 2023:1–170.
32. Pohan DJ, Marantuan RS, Djojosaputro M. Toxicity Test of Strong Drug Using the BSLT (Brine Shrimp Lethality Test) Method. Int J Heal Sci Res. 2023; 13(2):203–209.
33. Desviana L, Teruna HY, Jasril. Synthesis and Spectrum Analysis of Pyrazoline Compounds from Chalcone 4-Chloro Naphthalene. J Phot. 2015; 6(1):107–110.
34. Gupta R and Jain A. ChemInform Abstract: Improved Synthesis of Chalcones and Pyrazolines Under Ultrasonic Irradiation. ChemInform. 2018; 41(30):351-355.
35. Morais CS, Mengarda AC, Miguel FB, Enes KB, Rodrigues VC, Espírito-Santo MCC, Vieira JLB, Smaniotto MA,

Catenacci FS, Guimarães A, Ferraz L, Campos FML, Mendes IC, D'Oca MGM, Gnoatto SCB, Mendes MA, Barral-Netto M, Smaiotto MA. Pyrazoline Derivatives as Promising Novel Antischistosomal Agents. Sci Rep. 2021; 11(1):23812.

36. Shekhar Yadav C, Azad I, Rahman Khan A, Nasibullah M, Ahmad N, Hansda D, Ahsan F, Kumar A. Recent Advances in the Synthesis of Pyrazoline Derivatives from Chalcones as Potent Pharmacological Agents: A Comprehensive Review. Results Chem. 2024; 7:101326.
37. Farooq S, Ngaini Z, Mortadza NA. Microwave-Assisted Synthesis and Molecular Docking Study of Heteroaromatic Chalcone Derivatives as Potential Antibacterial Agents. Bull Korean Chem Soc. 2020; 41(6):592-598.
38. Mahmood Jawad A, Mohamed Salih MN, Helal TA, Hussein Obaid N, Mahmood Aljamali N. Review on Chalcone (Preparation, Reactions, Medical and Bio Applications). Int J Chem Synth Chem React. 2019; 5(1):1-10.
39. Tok F, Doğan MO, Gürbüz B, Baltaş S, Akdemir MN, Alp C. Synthesis of Novel Pyrazoline Derivatives and Evaluation of Their Antimicrobial Activity. J Res Pharm. 2022; 26(1):15-27.